Network pharmacology-based analysis and *in vitro* experimental verification of the inhibitory role of luteoloside on gastric cancer cells via the p53/p21 pathway

XIN-XING LIN[1*], PEI-QING YANG[2*], XIAO-JUN LI[1], ZHONG-ZHEN XU[2], HAI-TAO WU[1], SHUN-MING HU[2], XIAO-LEI YANG[1], YONG DING[1] and WEI-ZHOU YU[2]

[1]Department of General Surgery, Dafeng People's Hospital, Yancheng, Jiangsu 224100, P.R. China; [2]Department of Gastroenterology, Dafeng People's Hospital, Yancheng, Jiangsu 224100, P.R. China

Received April 9, 2024; Accepted August 16, 2024

DOI: 10.3892/ol.2024.14822

Abstract. The present study aimed to investigate the inhibitory effect of luteoloside on the proliferation, migration and invasion of gastric cancer (GC) cells based on network pharmacology and *in vitro* experiments. GC-associated targets were obtained from the GeneCards and Online Mendelian Inheritance in Man databases. Gene Ontology functional enrichment analysis and Kyoto Encyclopedia of Genes and Genomes pathway enrichment analysis were performed using the Database for Annotation, Visualization and Integrated Discovery. Protein-protein interaction (PPI) networks and herb-active ingredient-target gene-signaling pathway networks were constructed using the Search Tool for the Retrieval of Interacting Genes and proteins and Cytoscape software to analyze core target genes and pathways. In addition, the alkaline comet assay was performed to assess DNA damage, demonstrating that luteoloside induces DNA double-strand breaks in a concentration-dependent manner, as indicated by increased comet tail lengths. γ-H2AX detection through western blot analysis further corroborated these findings, showing significant upregulation of this DNA damage marker in luteoloside-treated GC cells. The human GC cell line NCI-N87 was utilized for *in vitro* experiments to investigate the impact of different doses of luteoloside on cell proliferation, invasion and migration using Cell Counting Kit-8, scratch-wound and Transwell assays, respectively. The underlying molecular mechanism of luteoloside was explored using western blot analysis. The successfully constructed PPI network revealed the p53, Akt1, Bcl-2 and Caspase-3 proteins as the core targets, all of which showed good binding activity with luteoloside. The *in vitro* experiments demonstrated that luteoloside treatment significantly inhibited GC-cell proliferation, migration and invasion. The western blot results showed notable concentration-dependent upregulation of p53 and p21 protein expression and downregulation of Bcl-2 protein expression following luteoloside treatment. Overall, luteoloside inhibited the proliferation, migration and invasion of GC cells by activating the p53/p21 signaling pathway.

Introduction

As one of the most common gastrointestinal tumors, gastric cancer (GC) has the 4th and 5th highest mortality and morbidity rates, respectively. A worldwide estimate of 769,000 fatalities from GC and >1 million new cases were reported in 2020 (1). Among malignant tumors in the Chinese population, the incidence and death rates of GC rank second and third, respectively (2,3). GC development is a complex process influenced by a variety of factors, including malnutrition, infections and genetics. Viruses (Epstein-Barr virus), bacteria (*Helicobacter pylori*) and inherited mutations in specific genes (GSTM1-null or CDH1 gene) may be the main risk factors for GC (4). In addition, lifestyle factors, such as nitroso-rich diets, alcohol consumption and smoking, are also associated with GC development (5). Currently, the basic treatment for GC is chemotherapy (6), but it has limited efficacy and serious side effects (6). Thus, identifying safe and available therapeutic drugs for GC treatment is urgent.

Natural herbs and their active ingredients, which have low toxicity and multiple targets, have recently demonstrated considerable potential as antitumor agents (7,8). Luteoloside, a natural flavonoid with diverse biological activities, is a main component of Ecliptae herba (9), also named 'Mo-Han-Lian', which is the dried aerial portion of *Eclipta prostrata* L. This plant is distributed throughout China (10) and possesses hypolipidemic (11), antitumor (12) and anti-inflammatory (13) properties due to its rich composition of bioactive compounds (14). Luteoloside also exerts pharmacological effects on the cardiovascular system and protective effects

Correspondence to: Dr Wei-Zhou Yu, Department of Gastroenterology, Dafeng People's Hospital, 139 Xingfu East Road, Dafeng, Yancheng, Jiangsu 224100, P.R. China
E-mail: weizhouyu2020@163.com

*Contributed equally

Key words: network pharmacology, luteoloside, gastric cancer, apoptosis, p53/p21 signaling pathway

on the neurological system (15), and possesses anti-inflammatory (16), antiviral (17) and anti-tumor properties (18). Furthermore, it has been demonstrated to block the proliferation and migration of human oral cancer cells by decreasing p38 phosphorylation and downregulating MMP-2 expression (19). Thus, luteoloside is of significant medical importance in cancer treatment.

To date, the influence of luteoloside on the proliferation, invasion and migration ability of GC cells has not been reported, to the best of our knowledge. In the present study, a network pharmacology-based strategy was used to determine the targets of the luteoloside associated with GC development. A protein-protein interaction (PPI) network was established and subsequently, a network topology was developed and functional enrichment analyses were performed. Finally, the mechanism of action of luteoloside was investigated using *in vitro* experiments, which validated the bioinformatics predictions by demonstrating the biological effects of luteoloside on GC cells, such as inhibiting their proliferation, migration and invasion. These results were consistent with the predicted involvement of the p53/p21 pathway and other molecular targets, thereby providing a theoretical reference for further experiments and the clinical use of luteoloside for GC treatment.

Materials and methods

Acquisition of GC target genes. The key word 'gastric cancer' was entered into the Online Mendelian Inheritance in Man (OMIM; https://omim.org/) and GeneCards (https://www.genecards.org/) databases to search for GC target genes. After compiling the results and removing duplicates, the remaining targets were uploaded to the UniProt database (https://www.uniprot.org/) to retrieve the names of the corresponding genes that are implicated in GC. After confirming the gene names in UniProt, they were reuploaded into the GeneCards database to cross-verify their specific roles and relevance in GC.

Acquisition of luteoloside target genes. The relevant targets and 3D structures of luteoloside were obtained from PubChem (https://pubchem.ncbi.nlm.nih.gov/), and potential targets from compound structures were predicted using SwissTargetPrediction (http://swisstargetprediction.ch/) and SuperPred (https://prediction.charite.de/index.php). In addition, the STITCH (http://stitch.embl.de/) database was used to predict genes that interact with the compounds.

Determination of the common targets between luteoloside and GC. The potential targets of luteoloside and the targets of GC were uploaded to Venny v2.1.0 (https://bioinfogp.cnb.csic.es/tools/venny/index.html) to create a Venn diagram to identify the common targets and the compounds corresponding to the common targets. The intersecting targets indicated those that luteoloside may act on GC.

Enrichment analyses. The Database for Annotation, Visualization and Integrated Discovery (DAVID; https://david.ncifcrf.gov/) was used to perform Kyoto Encyclopedia of Genes and Genomes (KEGG) pathway enrichment analysis and Gene Ontology (GO) functional enrichment analysis of the common targets between luteoloside and GC. The GO functional enrichment included the following categories: Molecular function (MF), cellular component (CC) and biological process (BP). The screening criteria were $P<0.01$, overlap ≥3 and enrichment ≥1.5. The enrichment results in the categories BP, CC and MF were plotted as bar graphs and the top 20 KEGG analysis results were plotted as a bubble chart.

Establishment of core target and PPI networks. The common targets between luteoloside and GC were uploaded to the STRING database (https://string-db.org/) and Cytoscape v3.8.0 software was used for visualization, where the option of 'Multiple protein' was selected, the protein species was set as '*Homo sapiens*', the confidence was set as 'highest confidence (≥0.900)' and the other parameters were kept at the default settings, resulting in the generation of a network diagram and data on the protein interactions with the highest correlation. The data were saved in TSV format. The Analyze Network tool in Cytoscape v3.8.0 software was used to construct the PPI network of luteoloside in the treatment of GC. Network analysis identified the pathways with the greatest involvement and these were considered the main signaling pathways of luteoloside in the treatment of GC.

Molecular docking. 3D structures of proteins were obtained from the Protein Data Bank (https://www.rcsb.org/). In addition, PyMOL version 2.4 (https://pymol.org/2/) was used for eliminating hydrogenated and excess ligands and water molecules, AutoDock version 4.2.6 (http://autodock.scripps.edu/) for molecular docking and Discovery Studio version 4.5 (https://discover.3ds.com/discovery-studio-visualizer-download) for visualizing the docking results. Binding energies <0 are generally considered to indicate the spontaneous binding of two molecules, with smaller binding energies indicating a more stable conformation.

Cell culture and grouping. The human GC cell line NCI-N87 (CRL-5822) was purchased from the American Type Culture Collection and incubated in RPMI-1640 medium (cat. no. R8758; Sigma-Aldrich; Merck KGaA) with 10% fetal bovine serum (cat. no. 16000-044; Gibco; Thermo Fisher Scientific, Inc.) and 1% penicillin-streptomycin at 37˚C in a humidified atmosphere containing 5% CO_2. Upon reaching 70-80% confluence, the cultured cells were partitioned into four groups as follows: i) Control group: NCI-N87 cells cultured under normal conditions; ii) low-concentration group: 25 μM luteoloside added to the NCI-N87 cell culture; iii) medium-concentration group: 50 μM luteoloside added to the NCI-N87 cell culture; and iv) high-concentration group: 100 μM luteoloside added to the NCI-N87 cell culture. The concentrations were chosen based on preliminary dose-response experiments and luteoloside (>98% purity) was purchased from Sigma-Aldrich (Merck KGaA).

Determination of cell proliferation. A Cell Counting Kit-8 (CCK-8; cat. no. 96992; Sigma-Aldrich; Merck KGaA) assay was used to determine the level of cell proliferation as per the manufacturer's instructions. In brief, cells from the different treatment groups were inoculated in a 96-well plate ($5x10^3$ cells/well) and complete medium (100 μl) was added to

each well. In the Cell Counting Kit-8 (CCK-8) assay, luteoloside was added to the culture medium at varying concentrations (25, 50 and 100 μM) before the 24-h incubation period, ensuring its presence during the entire experiment. Finally, the optical density of each well at 450 nm was measured using a microplate plate reader.

Determination of cell invasion. Transwell inserts (cat. no. 3422; Corning, Inc.) placed in 24-well plates and Matrigel® (cat. no. 354230; Corning, Inc.) were used to determine the levels of cell invasion. As per the manufacturer's instructions, Matrigel® (1:30) was applied to the porous membrane of the upper chamber and incubated for 1 h at 37˚C for solidification. Next, cell suspensions were inoculated in the upper chamber ($5x10^4$ cells/well), while 600 μl of complete medium was introduced into the lower chamber, and the cells were cultured for 24-48 h. The cells were then fixed with pre-cooled methanol at 4˚C for 15 min and rinsed with PBS. After this, the cells on the upper side of the membrane were carefully wiped off using a cotton swab, ensuring only the cells that had invaded to the lower side remained. Next, 0.1% crystal violet staining solution was added to the lower side of the membrane and incubated at room temperature for 30 min. The chambers were rinsed with PBS to remove the staining solution. The lower side of the membrane was photographed so that the number of cells that had passed through the Matrigel and the porous Transwell membrane could be counted. The results were analyzed using ImageJ software (version 1.53; National Institute of Health).

Determination of cell migration. A scratch-wound assay was performed to determine the extent of cell migration. First, cells were seeded in a 6-well plate at a density of $5x10^5$ cells/well. Once a monolayer had formed, a sterile 200-μl pipette tip was used to make a linear scratch on the monolayer. The cell surface was then washed with PBS to remove any cell debris generated from the scratch. After adding an appropriate amount of complete medium (with serum) (20), the culture was continued. After incubation for 24 h, the width of the scratch was photographed using an inverted microscope. The cell migration rate was calculated by comparing the initial width of the scratch with the width at the end of the incubation period. The results were analyzed using ImageJ software (version 1.53).

Alkaline comet assay. In brief, cells at a density of $1x10^5$/well were digested with 0.25% trypsin (Gibco; Thermo Fisher Scientific, Inc.). After centrifugation (2,000 x g, 4˚C, 5 min), the single-cell suspension was collected, mixed at a ratio of 1:10 with 1% low-melting-point agarose (Sigma-Aldrich; Merck KGaA) (37˚C) and the suspension (30 μl) was immediately transferred to a clean slide. The slides were placed flat in a light-proof environment at 4˚C for 10 min and then immersed in precooled 1X mammalian lysis buffer (Gibco; Thermo Fisher Scientific, Inc.) to completely cover the cells and gel and incubated overnight at 4˚C. The slides were then immersed in sodium alcohol ether sulfates (AES) for 1 h at 4˚C to unwind the DNA. Pre-cooled AES was added to the electrophoresis gel tray and the slides were immersed in the AES and electrophoresed at 30 V and 400 mA for 30 min. Subsequently, the slides were dried at 37˚C for 15 min and stained using 50 μl of red fluorescent nucleic acid staining solution (Invitrogen; Thermo Fisher Scientific, Inc.) at room temperature for 15 min in the dark. Finally, the slides were observed using fluorescent microscopy, and images were recorded and quantitatively analyzed using ImageJ software (version 1.53). The tail moment was calculated as the product of the tail length and Tail%DNA divided by 100. Tail%DNA refers to the percentage of DNA present in the comet tail relative to the total DNA in the comet, which includes both the tail and the head.

Western blot analysis of key signaling pathway-related proteins. Total protein of each group of cells was extracted using RIPA lysis buffer (Invitrogen; Thermo Fisher Scientific, Inc.) and quantified using a bicinchoninic acid assay kit (P1250-50; Applygen Technologies, Inc.) according to the manufacturer's instructions. Subsequently, 30 μg of the extracted total protein was separated by SDS-PAGE (10% polyacrylamide gel). Next, the gel was transferred to a polyvinylidene difluoride (PVDF) membrane (MilliporeSigma) and blocked for 1 h using a 5% solution of skimmed milk powder (Sigma-Aldrich; Merck KGaA). The membrane was incubated at 4˚C overnight with the following primary antibodies: γ-H2A histone family member X (γH2AX; cat. no. ab26350; 1:1,000 dilution; Abcam), p53 (cat. no. ab26; 1:1,000 dilution; Abcam), p21 (cat. no. ab109520; 1:1,000 dilution; Abcam), Bcl-2 (cat. no. ab182858; 1:1,000 dilution; Abcam) and β-actin (cat. no. ab8226; 1:5,000 dilution; Abcam). After rinsing in PBS, the membranes were incubated at ambient temperature for 1 h with the corresponding horseradish peroxidase (HRP)-labeled secondary antibodies; either HRP-labeled anti-rabbit IgG (cat. no. 7074; Cell Signaling Technology, Inc.) or HRP-labeled anti-mouse IgG (cat. no. 7076; Cell Signaling Technology, Inc.). The immunoblotting signals were developed using an enhanced chemiluminescence substrate (cat. no. 32106; Thermo Fisher Scientific, Inc.). Finally, the PVDF membrane were scanned with a chemiluminescence imaging system (ChemiDoc™ XRS+ System; Bio-Rad Laboratories, Inc.) and ImageJ software (version 1.53) was used to analyze the grayscale value of each protein band.

Statistical analysis. Statistical analysis was performed using SPSS 22.0 software (IBM Corp.). Quantitative data were expressed as the mean ± standard deviation. One-way analysis of variance followed by Tukey's post-hoc test was used to compare multiple groups. $P<0.05$ was considered to indicate a statistically significant difference.

Results

Screening of targets related to luteoloside and GC and analyses of GO functional enrichment and KEGG pathway enrichment. The target genes of luteoloside and GC-related genes obtained from relevant databases were screened to explore the mechanism of action of luteoloside in treating GC. A total of 3,514 and 10,778 GC-related targets were obtained from GeneCards and OMIM, respectively. After removing duplicates, a total of 11,482 GC-related genes remained. Potential targets of luteoloside were predicted using PubChem, SwissTargetPrediction and SuperPred, and genes

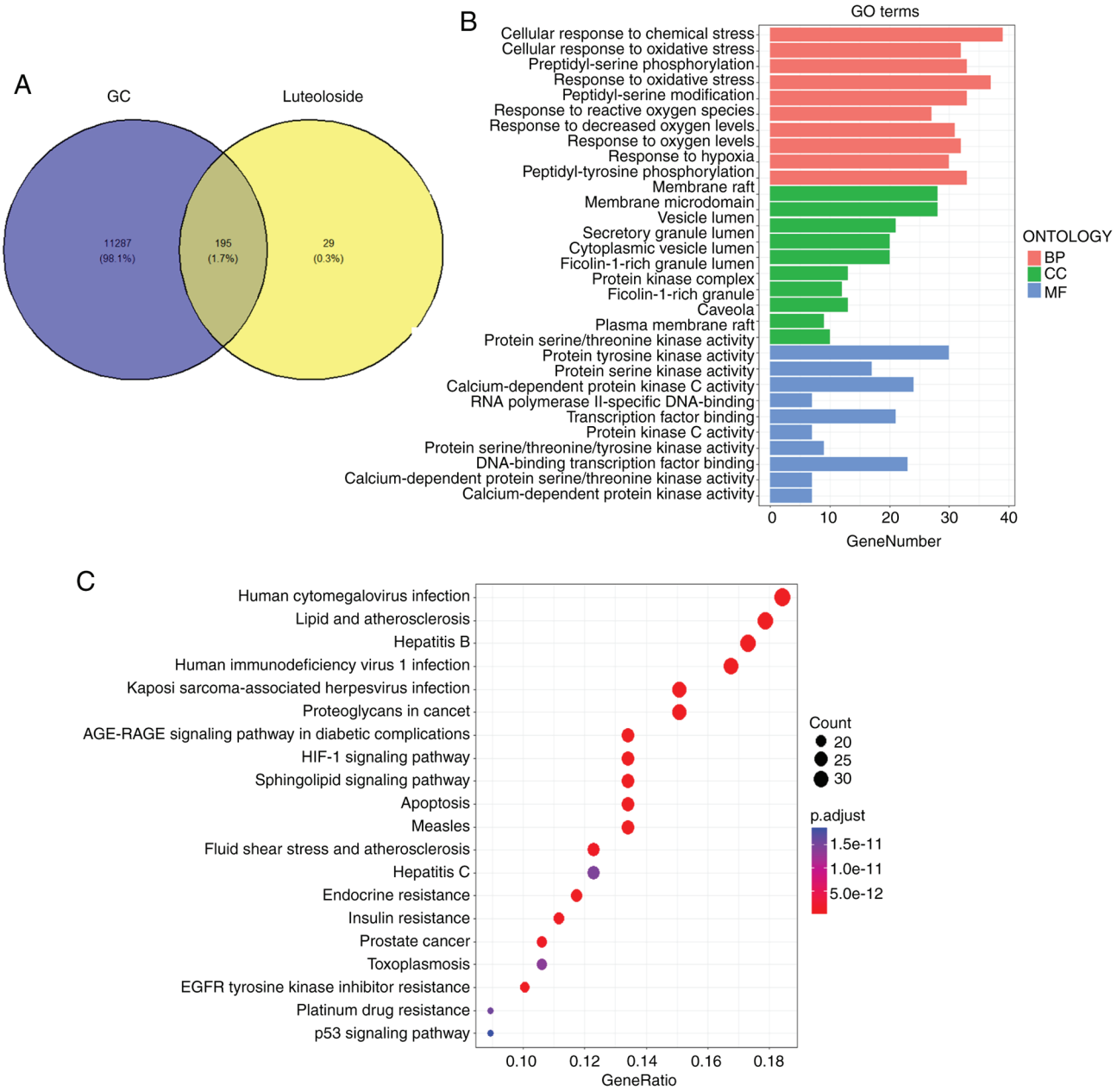

Figure 1. Screening of targets related to luteoloside and GC and analyses of GO functional enrichment and KEGG pathway enrichment. (A) The intersection of 224 luteoloside target genes and 11,482 GC-related genes using a Venn diagram revealed a total of 195 common action targets; (B) GO enrichment analysis results showing the top 10 BP, CC and MF terms associated with the common target genes of luteoloside and GC; (C) KEGG pathway enrichment analysis of molecular signaling pathways enriched for common target genes of luteoloside and GC. GC, gastric cancer; GO, Gene Ontology; KEGG, Kyoto Encyclopedia of Genes and Genomes; BP, biological process; CC, cellular component; MF, molecular function.

interacting with luteoloside were predicted using the STITCH database, resulting in a total of 224 targets in the dataset after removing duplicates. Venn diagram analysis of the intersection of luteoloside target genes and GC-related genes revealed 195 common targets of luteoloside in the treatment of GC (Fig. 1A), suggesting that they may be related to the treatment of GC with luteoloside.

Using the DAVID online database, the 195 common target genes underwent GO functional enrichment and KEGG pathway enrichment analyses. Fig. 1B shows the top 10 GO enrichment results. Enriched functional terms in the category BP mainly included 'negative regulation of apoptosis', 'protein phosphorylation' and 'signal transduction'; in the category CC, enriched functional terms were mainly cell structures such as the 'plasma membrane', 'cytoplasm' and 'cytosol'; and enriched functional terms in the category MF mainly included 'ATP binding', 'protein serine/threonine/tyrosine kinase activity' and 'protein kinase activity' (Fig. 1B). KEGG enrichment analysis revealed that the 195 common target genes were mostly enriched in pathways including hypoxia-inducible factor (HIF)-1 signaling, apoptosis, lipids and atherosclerosis, and p53 signaling (Fig. 1C). Overall, luteoloside may exert a therapeutic effect on GC by regulating these signaling pathways.

PPI network construction and core target gene screening. PPI analysis of the 195 common target genes of luteoloside

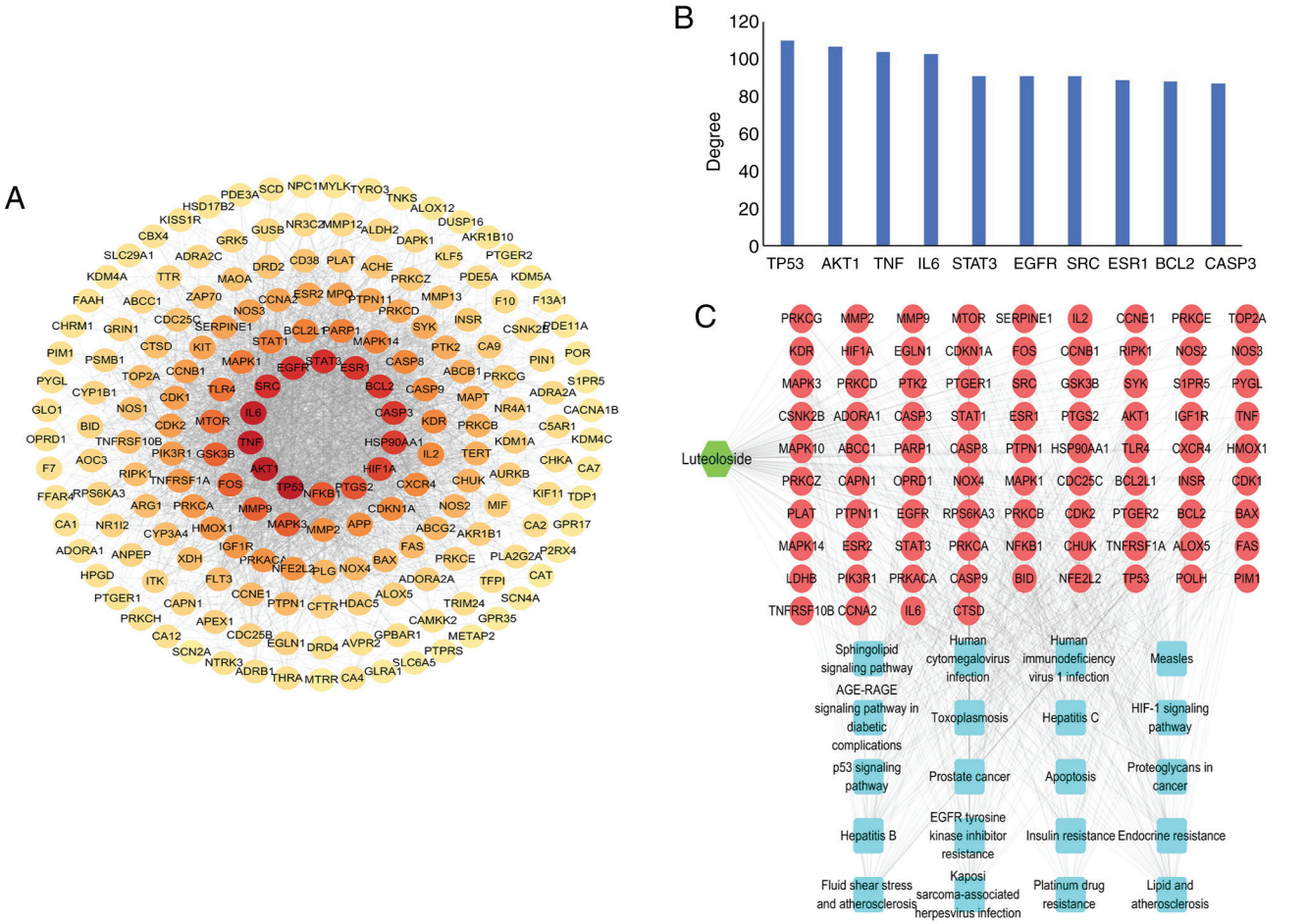

Figure 2. PPI network construction and core target gene screening. (A) PPI network of 195 common target genes between luteoloside and GC. The darkness of the node color reflects the importance of genes in the network. (B) Top 10 target genes in the PPI network. (C) Construction of a luteoloside-target-signaling pathway network. Red boxes indicate the active ingredients, blue oval nodes indicate the relevant target genes and green ovals indicate the top Kyoto Encyclopedia of Genes and Genomes signaling pathways. PPI, protein-protein interaction; GC, gastric cancer.

Table I. Molecular docking binding energies of active ingredients of luteoloside and key targets.

Protein (PDB structural identifier)	Affinity, kcal/mol
TP53 (1AIE)	-7.5
AKT1 (1H10)	-6.9
BCL2 (1G5M)	-8.5
CASP3 (1NME)	-6.9

TP53, tumor protein 53; CASP, caspase; AKT1, AKT serine/threonine kinase 1; PDB, Protein DataBank.

and GC was performed using the STRING database, and the PPI network of luteoloside in the treatment of GC was then constructed (Fig. 2A). The top 10 genes ranked by degree value were, in order, tumor protein (*TP*)*53*, threonine kinase 1 (*AKT1*), *TNF*, *IL6*, *STAT3*, *EGFR*, *SRC*, *ESR1*, *BCL2* and caspase (*CASP*)*3* (Fig. 2B). The high degree values suggested that these genes have key roles in the PPI network. A luteoloside-target-signaling pathway network was also constructed (Fig. 2C); the 20 most significant pathways from the KEGG enrichment analysis were obtained, and the 10 genes with the largest degree among them were analyzed. After intersection, four common genes (*TP53*, *AKT1*, *BCL2* and *CASP3*) were identified.

Molecular docking of p53, Akt1, Bcl-2 and Casp3 with luteoloside. AutoDock was used for the molecular docking of luteoloside and key targets. Luteoloside was docked with the top four targets: p53, Akt1, Bcl-2 and Casp3. Table I shows the intermolecular docking binding energies and the molecular docking conformation of luteoloside is presented in Fig. 3. The results were visualized using PyMOL and showed good matching. The optimal conformation of compound-target binding was presented in the form of hydrogen bonding and the binding energy was <-6.0 kcal/mol, indicating high binding activity.

Luteoloside inhibits the proliferation, invasion and migration of NCI-N87 cells. The CCK-8 assay was used to explore the role of luteoloside in NCI-N87 cells and the impact of different concentrations on cell proliferation (Fig. 4A). Compared with the control cells, the proliferation of NCI-N87 cells treated with luteoloside showed a dose-dependent decrease as the luteoloside concentration increased. The invasion ability of

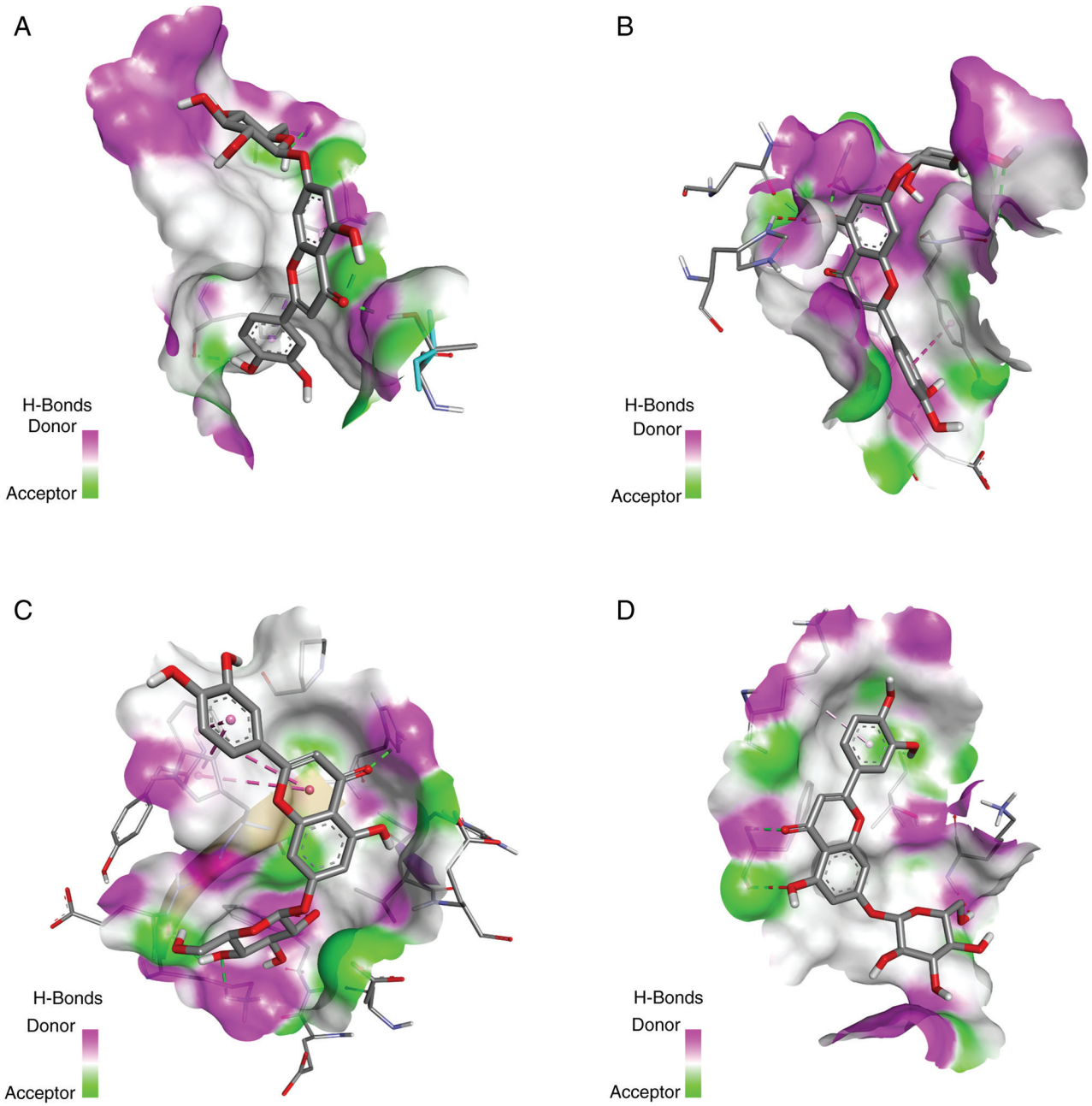

Figure 3. Molecular docking of p53, Akt1, Bcl-2 and Casp3 with luteoloside. (A) Luteoloside-p53; (B) luteoloside-Akt1; (C) luteoloside-Bcl-2; (D) luteoloside-Casp3. Casp, caspase; AKT1, AKT serine/threonine kinase 1.

NCI-N87 cells in each group was explored using the Transwell assay (Fig. 4B). Luteoloside treatment visibly inhibited the invasive ability of NCI-N87 cells. The influence of various concentrations of luteoloside on the migration of NCI-N87 cells was investigated using the scratch-wound assay (Fig. 4C). Compared with the control group, luteoloside treatment significantly decreased the migration ability of NCI-N87 cells. The above results indicated the potential of luteoloside to inhibit the proliferation, invasion and migration of NCI-N87 cells.

Luteoloside promotes DNA damage in NCI-N87 cells. The comet assay was performed to determine whether luteoloside is able to induce DNA double-strand breaks (DSBs). Luteoloside treatment increased the length of comet tails in NCI-N87 cells, which was further enhanced with increasing concentrations, suggesting that luteoloside contributed to the induction of cellular DNA damage (Fig. 5A). The effect of luteoloside on DNA damage marker γH2AX in NCI-N87 cells was also evaluated. Western blot analysis showed that the protein level of γH2AX was significantly elevated in NCI-N87 cells in a concentration-dependent manner relative to the control group (Fig. 5B). Collectively, these findings indicated that luteoloside induced DNA DSBs, as evidenced by elevated γH2AX protein levels and enhanced comet tail moments.

Luteoloside activates the p53/p21 pathway in NCI-N87 cells. The expression of p53/p21 signaling pathway-related proteins was analyzed in conjunction with the preceding bioinformatics results. Western blot analysis showed that, compared with the control group, p53 and p21 levels increased with increasing

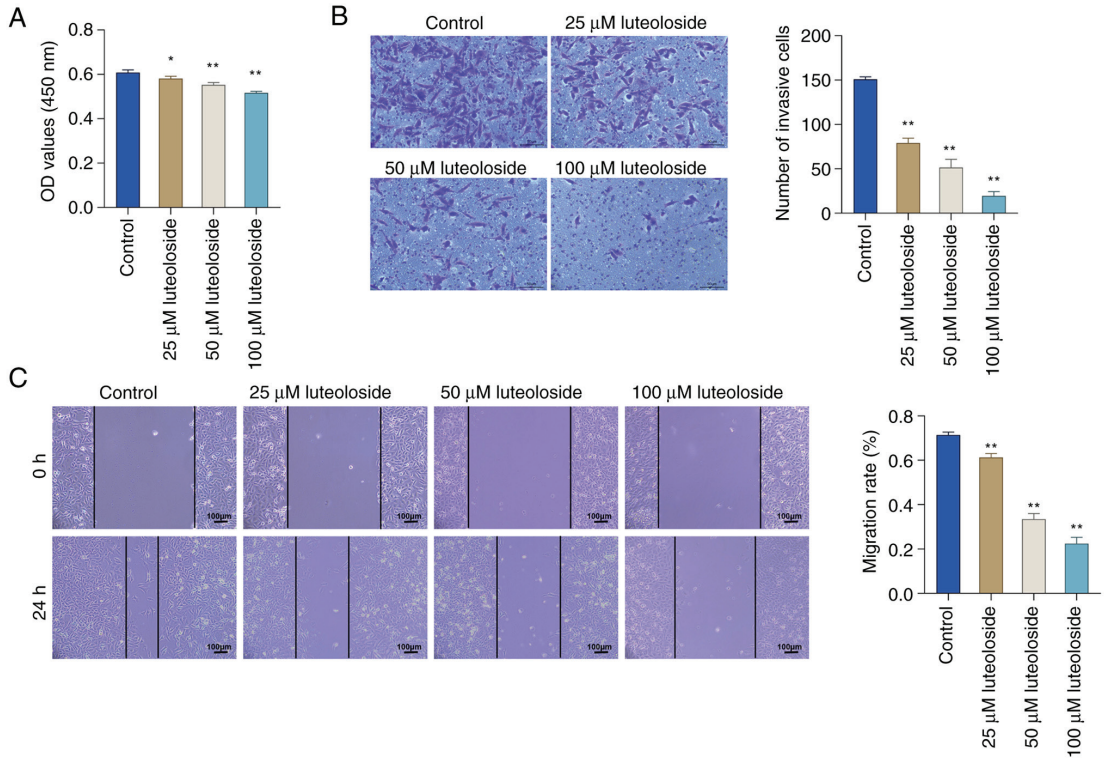

Figure 4. Luteoloside inhibits the proliferation, invasion and migration of human gastric cancer NCI-N87 cells. (A) Cell Counting Kit-8 assay using a microplate reader in the final step to measure the OD_{450} of each well as an indicator of cell proliferation. (B) Transwell assay to determine the effect of luteoloside treatment on NCI-N87-cell invasion (scale bars, 50 μm). (C) Scratch-wound assay to determine the migration ability of NCI-N87 cells (scale bars, 100 μm). *P<0.05, **P<0.01 vs. the control group. OD_{450}, optical density at 450 nm.

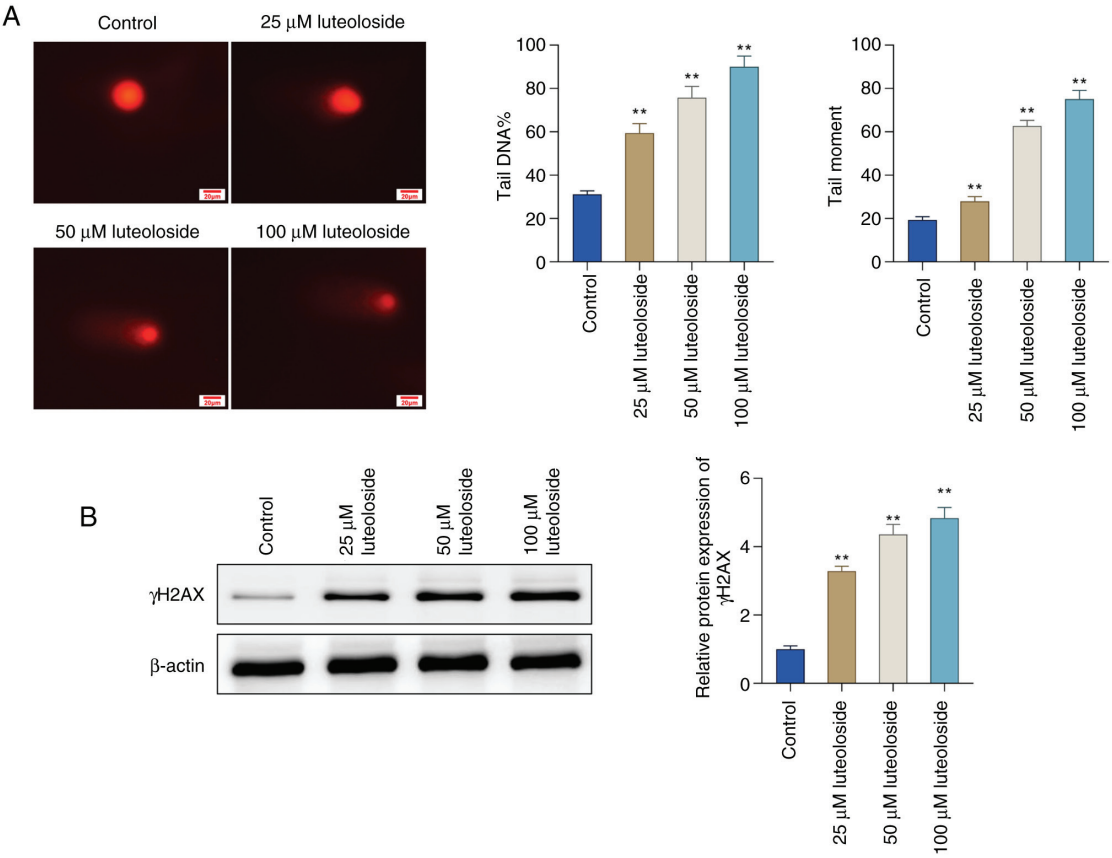

Figure 5. Luteoloside promotes DNA damage of human gastric cancer NCI-N87 cells. (A) Representative comet analysis images and quantification of comet tail DNA levels and tail moment using the OpenComet plugin for ImageJ (scale bars, 20 μm). (B) Effect of luteoloside on γH2AX protein levels in NCI-N87 cells determined by western blot analysis. **P<0.01 vs. the control group.

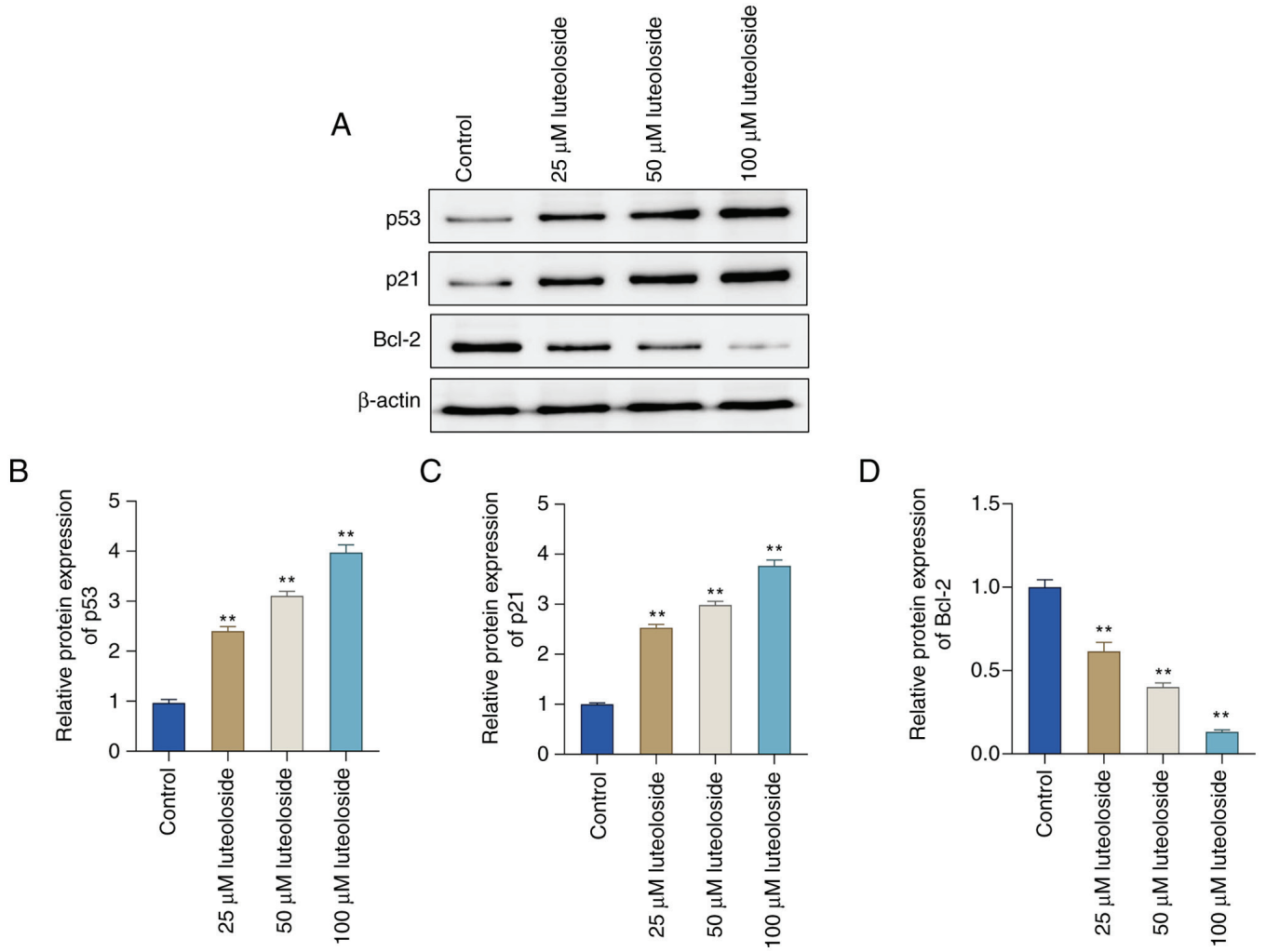

Figure 6. Luteoloside activates the p53/p21 pathway in human gastric cancer NCI-N87 cells. (A) Western blot analysis was performed to detect the relative expression levels of p53, p21 and Bcl-2 in NCI-N87 cells in each group; (B) quantified expression levels of p53; (C) quantified expression levels of p21; (D) quantified expression levels of Bcl-2. **P<0.01 vs. the control group.

concentrations of luteoloside. However, Bcl-2 levels showed a concentration-dependent decrease after luteoloside treatment (Fig. 6A-D). Collectively, these results indicated that the p53/p21 signaling pathway has a key role in luteoloside-induced inhibition of GC cell invasion, migration and proliferation.

Discussion

Gastric cancer (GC) is a leading cause of cancer-related deaths globally, with limited treatment options due to the severe side effects and limited efficacy of existing chemotherapies. In the present study, the intersection of 195 common targets of luteoloside and GC was identified. PPI network analysis showed that p53, Akt1, Bcl-2 and Casp3 were the core targets for luteoloside treatment of GC, and they all showed good binding activity with luteoloside. GO functional enrichment and KEGG pathway enrichment analyses revealed that luteoloside exerted anti-GC effects through various signals, including 'negative regulation of apoptosis', 'lipids' and 'atherosclerosis', 'HIF-1 signaling' and 'p53 signaling'. These signaling pathways have been reported to inhibit GC growth by regulating several tumor development processes, including angiogenesis, proliferation, apoptosis, metastasis and invasion of human GC cells (21-23). Among them, apoptosis is one of the most important, and triggering apoptosis in cancer cells has received attention as a potential treatment for GC (21,24-26).

On the basis of the present networks pharmacology findings, *in vitro* experiments were first performed to investigate the effects of different concentrations of luteoloside on GC cells. The CCK-8 assay results revealed that luteoloside significantly decreased the rate of proliferation of GC cells. The Transwell and scratch-wound assay results indicated that luteoloside considerably reduced the invasion and migration capabilities of GC cells, respectively. Therefore, it may be suggested that luteoloside may serve as a therapeutic agent for GC by successfully preventing the proliferation, migration and invasion of GC cells. Next, the mechanism of action of luteoloside in GC cells was further explored. p53 is a tumor suppressor protein and its most important pathway for tumor suppression is the induction of apoptosis and cell cycle arrest (27). p53 significantly promotes the transcriptional activity of the cell cycle regulator p21, and the p53/p21 signaling pathway is a central regulatory pathway that controls cell-cycle progression and regulates apoptosis

in tumor cells (28,29). Bcl-2 is an anti-apoptotic protein. p53 binds to Bcl-2 family proteins to release Bax, which exerts anti-invasive or proapoptotic effects, depending on the stress environment (30). In the *in vitro* experiments of the present study, p53 and p21 protein expression levels were markedly upregulated and Bcl-2 protein expression was notably downregulated in GC cells after luteoloside treatment in a concentration-dependent manner. These findings suggest that luteoloside promotes GC-cell apoptosis by activating the p53/p21 signaling pathway, thereby suppressing GC-cell invasion, proliferation and migration. It is important to note that the NCI-N87 cell line possesses a p53 missense mutation (p.Arg248Gln), which is pathogenic and common in gastric cancer. Despite this mutation, luteoloside was still able to activate the p53/p21 signaling pathway, indicating that the inhibitory effects on cell proliferation, migration and invasion are relevant even in the presence of such mutations.

Signaling pathways of research significance were screened and it was verified that luteoloside effectively hindered 'GC-cell proliferation', migration and invasion. However, the impact on proliferation was not as pronounced as its effects on migration and invasion. This could potentially be attributed to the doubling time of the cell line, which may influence the observed effects within the 24-h period. In addition, apoptosis, which reduces the number of viable cells, tends to occur after 24 h, suggesting that more pronounced effects on proliferation may become evident over longer incubation periods. In additionally, there are certain limitations to the present study. Previous *in vivo* studies have demonstrated that luteoloside exhibits various beneficial effects, such as analgesic and neuroprotective properties, although these outcomes were achieved at different doses than those applied in the present study (31,32). For instance, luteoloside has been shown to reduce pain and protect against neuronal damage in animal models, indicating its potential therapeutic applications. However, to translate these findings into the context of gastric cancer, *in vivo* experiments are essential to verify whether luteoloside can exert similar therapeutic effects on gastric cancer at the appropriate doses. First, *in vivo* experiments are necessary to verify the therapeutic effect of luteoloside on GC. Furthermore, the involvement of p53/p21 signaling in the luteoloside-induced inhibition of GC cells requires verification by gene knockout or a similar process. Alternatively, an *in vitro* rescue experiment, where p53/p21 is silenced or inhibited using small inhibitory RNA or specific inhibitors, followed by luteoloside treatment, could assess whether the inhibition of GC cell proliferation, migration and invasion is reversed. This would provide functional insights and be less time-consuming than gene knockout, making it a practical approach to validate the pathway's role.

In this study, the NCI-N87 gastric cancer cell line was utilized, which harbors a p53 missense mutation (p.Arg248Gln) known to be pathogenic and common in gastric cancer. Of note, certain p53 mutations may not lead to a complete loss of function and the present findings demonstrate that luteoloside can still activate the p53/p21 signaling pathway in these cells. This suggests that even in the presence of a p53 mutation, luteoloside may exert its inhibitory effects on cell proliferation, migration and invasion through this pathway. This discovery highlights the potential of luteoloside as a therapeutic agent and indicates that the p53 pathway can be effectively activated even in gastric cancer cells with specific p53 mutations. Future research should further explore the mechanism of luteoloside in the context of different p53 mutation backgrounds.

The present study demonstrated that luteoloside significantly enhances cell migration in a scratch-wound assay, suggesting its potential role in wound healing. Previous studies have shown that luteoloside can inhibit the NF-κB pathway and induce apoptosis in cancer cells (33,34), which may suggest that its effects are dose-dependent and context-specific. However, the scratch-wound assay has limitations, as it does not fully replicate the complex *in vivo* environment. Although apoptosis was not observed in the present study within the 24-h incubation period, it is possible that apoptosis may occur with prolonged exposure. Future research should explore longer incubation times and investigate the underlying molecular mechanisms, particularly the potential involvement of NF-κB.

In conclusion, network pharmacology combined with *in vitro* experiments were used to confirm that luteoloside inhibits the proliferation, invasion and migration of GC cells by activating the p53/p21 signaling pathway. Thus, luteoloside is expected to be a promising therapeutic drug for GC.

Acknowledgements

Not applicable.

Funding

No funding was received.

Availability of data and materials

The data generated in the present study may be requested from the corresponding author.

Authors' contributions

XXL and PQY designed the study and drafted the manuscript. XJL, ZZX, SMH and HTW carried out the statistical analysis. XLY, YD and WZY participated in the study design, contributed to data collection and analysis, and confirmed the authenticity of all the raw data. SMH and XLY contributed to the discussion section and revised it critically for important intellectual content. All authors have read and approved the final manuscript.

Ethics approval and consent to participate

Not applicable.

Patient consent for publication

Not applicable.

Competing interests

The authors declare that they have no competing interests.

References

1. Sung H, Ferlay J, Siegel RL, Laversanne M, Soerjomataram I, Jemal A and Bray F: Global cancer statistics 2020: GLOBOCAN estimates of incidence and mortality worldwide for 36 cancers in 185 countries. CA Cancer J Clin 71: 209-249, 2021.
2. Cao MM, Li H, Sun DQ, He SY, Lei L, Peng J and Chen WQ: Epidemiological trend analysis of gastric cancer in China from 2000 to 2019. Chin J Dig Surg 20: 102-109, 2021.
3. Cao M and Chen W: Epidemiology of cancer in China and the current status of prevention and control. Chin J Clin Oncol 46: 145-149, 2019.
4. Rawla P and Barsouk A: Epidemiology of gastric cancer: Global trends, risk factors and prevention. Prz Gastroenterol 14: 26-38, 2019.
5. Kobayashi J: Effect of diet and gut environment on the gastrointestinal formation of N-nitroso compounds: A review. Nitric Oxide 73: 66-73, 2018.
6. Ilson DH: Advances in the treatment of gastric cancer: 2019. Curr Opin Gastroenterol 35: 551-554, 2019.
7. Li M, Wang MM, Guo XW, Wu CY, Li DR, Zhang X and Zhang PT: Different survival benefits of Chinese medicine for pancreatic cancer: How to choose? Chin J Integr Med 24: 178-184, 2018.
8. Jia W and Wang L: Using traditional Chinese medicine to treat hepatocellular carcinoma by targeting tumor immunity. Evid Based Complement Alternat Med 2020: 9843486, 2020.
9. Bouyahya A, Taha D, Benali T, Zengin G, El Omari N, El Hachlafi N, Khalid A, Abdalla AN, Ardianto C, Tan CS, *et al*: Natural sources, biological effects, and pharmacological properties of cynaroside. Biomed Pharmacother 161: 114337, 2023.
10. Jiao GY, Li SK, Deng Y, Yin J, Chen WS, Chen JF and Zhang F: Review of pharmacological effects, metabolism and quality control of *Eclipta prostrata* L. and its chemical components. J Pharm Res 40: 673-677, 683, 2021.
11. Gupta A, Kumar A, Kumar D, Nandan S, Shankar K, Varshney S, Rajan S, Srivastava A, Gupta S, Kanojiya S, *et al*: Ethyl acetate fraction of Eclipta alba: A potential phytopharmaceutical targeting adipocyte differentiation. Biomed Pharmacother 96: 572-583, 2017.
12. Yadav NK, Arya RK, Dev K, Sharma C, Hossain Z, Meena S, Arya KR, Gayen JR, Datta D and Singh RK: Alcoholic Extract of Eclipta alba shows in vitro antioxidant and anticancer activity without exhibiting toxicological effects. Oxid Med Cell Longev 2017: 9094641, 2017.
13. Ryu S, Shin JS, Jung JY, Cho YW, Kim SJ, Jang DS and Lee KT: Echinocystic acid isolated from *Eclipta prostrata* suppresses lipopolysaccharide-induced iNOS, TNF-α, and IL-6 expressions via NF-κB inactivation in RAW 264.7 macrophages. Planta Med 79: 1031-1037, 2013.
14. Timalsina D and Devkota HP: *Eclipta prostrata* (L.) L. (asteraceae): Ethnomedicinal uses, chemical constituents, and biological activities. Biomolecules 11: 1738, 2021.
15. Rehfeldt SCH, Silva J, Alves C, Pinteus S, Pedrosa R, Laufer S and Goettert MI: Neuroprotective effect of luteolin-7-O-glucoside against 6-OHDA-induced damage in undifferentiated and RA-differentiated SH-SY5Y cells. Int J Mol Sci 23: 2914, 2022.
16. Caporali S, De Stefano A, Calabrese C, Giovannelli A, Pieri M, Savini I, Tesauro M, Bernardini S, Minieri M and Terrinoni A: Anti-inflammatory and active biological properties of the plant-derived bioactive compounds luteolin and luteolin 7-glucoside. Nutrients 14: 1155, 2022.
17. Schonhofer C, Yi J, Sciorillo A, Andrae-Marobela K, Cochrane A, Harris M, Brumme ZL, Brockman MA, Mounzer K, Hart C, *et al*: Flavonoid-based inhibition of cyclin-dependent kinase 9 without concomitant inhibition of histone deacetylases durably reinforces HIV latency. Biochem Pharmacol 186: 114462, 2021.
18. Ji J, Wang Z, Sun W, Li Z, Cai H, Zhao E and Cui H: Effects of cynaroside on cell proliferation, apoptosis, migration and invasion though the MET/AKT/mTOR axis in gastric cancer. Int J Mol Sci 22: 12125, 2021.
19. Velmurugan BK, Lin JT, Mahalakshmi B, Chuang YC, Lin CC, Lo YS, Hsieh MJ and Chen MK: Luteolin-7-O-glucoside inhibits oral cancer cell migration and invasion by regulating matrix metalloproteinase-2 expression and extracellular signal-regulated kinase pathway. Biomolecules 10: 502, 2020.
20. Arora M: Cell culture media: A review. Mater Methods 3: 175, 2013.
21. Rong L, Li Z, Leng X, Li H, Ma Y, Chen Y and Song F: Salidroside induces apoptosis and protective autophagy in human gastric cancer AGS cells through the PI3K/Akt/mTOR pathway. Biomed Pharmacother 122: 109726, 2020.
22. Ji H and Zhang X: RPL38 regulates the proliferation and apoptosis of gastric cancer via miR-374b-5p/VEGF signal pathway. Onco Targets Ther 13: 6131-6141, 2020.
23. Pei J, Wei D and Jiang L: Effects of Yiqi huayu sanjie decoction on PI3K-AKT-mTOR signal pathway of gastric cancer cell line of SGC-7901. World Chin Med 15: 2686-2689, 2695, 2020.
24. Jeong S, Jo MJ, Yun HK, Kim DY, Kim BR, Kim JL, Park SH, Na YJ, Jeong YA, Kim BG, *et al*: Cannabidiol promotes apoptosis via regulation of XIAP/Smac in gastric cancer. Cell Death Dis 10: 846, 2019.
25. Liang JR and Yang H: Ginkgolic acid (GA) suppresses gastric cancer growth by inducing apoptosis and suppressing STAT3/JAK2 signaling regulated by ROS. Biomed Pharmacother 125: 109585, 2020.
26. Gao S, Tan H and Li D: Oridonin suppresses gastric cancer SGC-7901 cell proliferation by targeting the TNF-alpha/androgen receptor/TGF-beta signalling pathway axis. J Cell Mol Med 27: 2661-2674, 2023.
27. Mao Y and Jiang P: The crisscross between p53 and metabolism in cancer. Acta Biochim Biophys Sin (Shanghai) 55: 914-922, 2023.
28. Gu X, Wang Z, Gao J, Han D, Zhang L, Chen P, Luo G and Han B: SIRT1 suppresses p53-dependent apoptosis by modulation of p21 in osteoblast-like MC3T3-E1 cells exposed to fluoride. Toxicol In Vitro 57: 28-38, 2019.
29. Zhuang C, Zhao J, Zhang S and Shahid M: Escherichia coli infection mediates pyroptosis via activating p53-p21 pathway-regulated apoptosis and cell cycle arrest in bovine mammary epithelial cells. Microb Pathog 184: 106338, 2023.
30. Kim EM, Jung CH, Kim J, Hwang SG, Park JK and Um HD: The p53/p21 complex regulates cancer cell invasion and apoptosis by targeting Bcl-2 family proteins. Cancer Res 77: 3092-3100, 2017.
31. Nabavi SF, Braidy N, Gortzi O, Sobarzo-Sanchez E, Daglia M, Skalicka-Woźniak K and Nabavi SM: Luteolin as an anti-inflammatory and neuroprotective agent: A brief review. Brain Res Bull 119: 1-11, 2015.
32. Li Q, Tian Z, Wang M, Kou J, Wang C, Rong X, Li J, Xie X and Pang X: Luteoloside attenuates neuroinflammation in focal cerebral ischemia in rats via regulation of the PPARγ/Nrf2/NF-κB signaling pathway. Int Immunopharmacol 66: 309-316, 2019.
33. Park CM and Song YS: Luteolin and luteolin-7-O-glucoside inhibit lipopolysaccharide-induced inflammatory responses through modulation of NF-κB/AP-1/PI3K-Akt signaling cascades in RAW 264.7 cells. Nutr Res Pract 7: 423-429, 2013.
34. Lin J, Chen J, Zhang Z, Xu T, Shao Z, Wang X, Ding Y, Tian N, Jin H, Sheng S, *et al*: Luteoloside inhibits IL-1β-induced apoptosis and catabolism in nucleus pulposus cells and ameliorates intervertebral disk degeneration. Front Pharmacol 10: 868, 2019.